15 September, 2021

Minyan Wang (PhD)
Department of Biological Sciences
Director, Centre for Neuroscience
Xi'an Jiaotong-Liverpool University
SA451, 111 Ren'ai Road, Suzhou, 215123, China
Tel: +86 (0)512 88161662
Email: minyan.wang@xjtlu.edu.cn

Editor

J Headache Pain

Dear Professor Paolo Martelletti,

I write to submit the manuscript entitled 'Src family kinases activity is required for transmitting purinergic P2X7 receptor signaling in cortical spreading depression and neuroinflammation' to J Headache Pain for publication.

In this manuscript, we report that SFKs activity plays a key role in governing P2X7 receptor signaling in contributing to CSD propagation, CSD-induced cortical neuroinflammation and glutamate release. Our data unravels a novel mechanism by which P2X7 receptor signals via pore formation to SFKs, contributing to migraine pathogenesis. The data suggest that P2X7 receptor and SFKs, in particular Fyn kinase, can be used as potential targets in migraine prophylaxis and therapy.

We believe that our finding will be of general interest to the Headache and Pain field.

Thank you for considering this manuscript.

Sincerely,

Minyan Wang, Ph.D.
Senior Associate Professor, Dept. of Biological Sciences
Xi'an Jiaotong-Liverpool University

Src family kinases activity is required for transmitting purinergic P2X7 receptor signaling in cortical spreading depression and neuroinflammation

Abbreviated title: SFKs are required for P2X7R signaling during CSD and neuroinflammation

Lingdi Nie[1,2], Dongqing Ma [1,2], John P Quinn[2], Minyan Wang [1,2 §]

Author affiliations:

[1] Department of Biological Sciences, Centre for Neuroscience, Xi'an Jiaotong-Liverpool University (XJTLU), Suzhou, 215123, China

[2] Department of Pharmacology and Therapeutics, Institute of Systems, Molecular and Integrative Biology, Liverpool, L69 7ZB, UK.

[§] Corresponding author: Minyan Wang (PhD), SA451, Department of Biological Sciences, Xi'an Jiaotong-Liverpool University, 111 Ren Ai Road, Suzhou Industrial Park, Suzhou 215123, P.R. China. Phone: + 86 512 8816 1662. Email: Minyan.wang@xjtlu.edu.cn

Emails of other authors: Ms Lingdi Nie: lingdi.nie@xjtlu.edu.cn; Dr Dongqing Ma: Dongqing.Ma13@alumni.xjtlu.edu.cn; Professor John Quinn: jquinn@liverpool.ac.uk

Abstract

Background

Purinergic P2X7 receptor plays a key role in migraine pathophysiology. Yet precise molecular mechanism underlying P2X7R signaling in migraine remains unclear. This study explores the hypothesis that P2X7 receptor transmits signaling to Src family kinases (SFKs) during cortical spreading depression (CSD) and CSD-induced neuroinflammation.

Methods

CSD was recorded using electrophysiology in rats, and intrinsic optical imaging in mouse brain slices. Cortical IL-1β and TNFα mRNA expression were detected using qPCR. Glutamate release in mouse brain slices was detected using glutamate assay.

Results

The data showed that systematic deactivation of SFKs by PP2 reduced cortical susceptibility to CSD in rats and CSD-induced IL-1β and TNF-α gene expression in rat ipsilateral cortices. Consistently, in mouse brain slices, inhibition of SFKs activity by saracatinib and P2X7 receptor by A740003 similarly reduced cortical susceptibility to CSD. When the interaction of P2X7 receptor-SFKs was disrupted by TAT-P2X7, a marked reduction of cortical susceptibility to CSD, CSD-induced IL-1β gene expression and glutamate release were observed in mouse brain slices. The reduced cortical susceptibility to CSD by TAT-P2X7 was restored by NMDA and disrupting Fyn-NMDA interaction using TAT-Fyn (39-57), but not disrupting Src-NMDA receptor using TAT-Src (40-49), reduced cortical susceptibility to CSD. Furthermore, activation of P2X7 receptor by BzATP restored the TAT-Fyn (39-57)-reduced cortical susceptibility to CSD.

Conclusion

This study reveals that SFKs activity mediates P2X7 receptor pore formation facilitating CSD propagation, CSD-induced neuroinflammation and glutamate release, of particular relevance to migraine.

KEY WORDS

Migraine, cortical spreading depression, P2X7 receptor, Src family kinases, glutamatergic pathway

Background

Migraine is neurovascular disorder that is characterized by complicated pathophysiology, among which cortical spreading depression (CSD) is a key correlate leading to both central and peripheral sensitization [1]. CSD is a temporary propagating wave of depolarization followed by depression on cerebral cortex and subcortical regions [1]. CSD disrupts ionic homeostasis and induces release of adenosine triphosphate (ATP) [2] and neurotransmitters especially glutamate, calcitonin gene-related peptide (CGRP) and pituitary adenylate cyclase activating polypeptide (PACAP) [3], which subsequently result in aberrant cortical excitability. CSD also causes neuroinflammation via mast cell degranulation, release of inflammatory cytokines and increases cerebral and meningeal blood flow [4, 5]. All these result in the activation and sensitization of meningeal nociceptors and trigeminovascular system, which ultimately evoke the onset of migraine headache [6]. More recently, CSD is shown to induce facial hyperalgesia, photophobia and hypomotility in mice, supporting the role of CSD as a nociceptive stimulus underlying migraine with aura [7].

The molecular mechanisms underlying CSD-induced migraine is not fully understood but activation of membrane receptors and channels, of which N-methyl-D-aspartic acid (NMDA) receptors [8], gamma-Aminobutyric acid receptors [9], purinergic receptor P2X7 [10], transient receptor potential ankyrin 1 [11] and Pannexin-1 (Panx1) [4] have been well known to contribute to migraine pathogenesis. Of these, P2X7 receptor, a member of the purinergic receptor family that can be activated in response to ATP, has been increasingly drawn to the attention in that the receptor regulate a plethora of cellular signaling events in both central and peripheral nervous system [12]. P2X7 receptor possess an ion channel function and also opens a large transmembrane pore that is permeable to large hydrophilic molecules via forming a complex with Panx1 [13]. Recent findings on P2X7 receptor in migraine models suggest that P2X7 receptor contributes to migraine pathogenesis. In nitroglycerin (NTG)-induced mouse migraine model, inhibition of P2X7 receptor activity attenuates mechanical and thermal hyperalgesia, inflammatory response and central sensitization via promoting

autophagic process in trigeminal nucleus caudalis (TNC) [14, 15]; Whilst the recurrent NTG in turn increases P2X7 receptor protein expression in TNC [15]. In the CSD-induced migraine model, inhibition of P2X7 receptor pore formation attenuates cortical susceptibility to CSD, CSD-induced neuroinflammation and trigeminovascular activation [10]. Despite that P2X7 receptor plays a crucial role in migraine progression, the underlying migraine mechanism by which P2X7 receptor transmits signaling remains unclear.

As an intracellular signaling molecule, Src family kinases (SFKs) have an identified interaction with P2X7 receptor in various cell models. P2X7 receptor physically interacts with SFKs whilst activation of P2X7 receptor increases phosphorylated SFKs level at the tyrosine 416 site in J774 macrophages [16]. Functionally, deactivation of SFKs reduces both P2X7 receptor-induced pore formation [16] and morphine-induced P2X7 receptor-mediated currents and Ca^{2+} responses [17]. SFKs also regulate P2X7 receptor-mediated IL-1 release and reactive oxygen species production via p38 mitogen-activated protein kinase (MAPK) in glial cells [18, 19] and extracellular-signal-regulated kinase 1/2 activation in macrophage [19]. Taken the above evidence and given that activation of SFKs is required for CSD propagation [20, 21] and is proposed as an emerging target for migraine therapy [22], it is likely that SFKs are a key mediator downstream of P2X7 receptor to facilitate migraine progression.

Here we examined the hypothesis that activation of SFKs is required for P2X7 receptor signaling in mediating CSD and CSD-induced cortical neuroinflammation. The involvement of glutamatergic pathway in P2X7 receptor/SFKs signaling during CSD was also explored. Our data unravels that P2X7 receptor signals to SFKs, which activation facilitates CSD propagation and CSD-induced neuroinflammation.

Methods

Animals

A total of 35 adult male Sprague-Dawley rats (311.6 ± 6.8 g), 54 adult male C57BL/6J mice (20.9 ± 0.27 g) or 22 adult male Balb/c mice (21.6 ± 0.3 g) were purchased from

Shanghai SLAC Laboratory Animal Corporation Ltd. Only the males were used in this study so as to minimize any potential impact of fluctuating levels of hormones in females. Animal experiments were carried out under ethic approval by Jiaotong-Liverpool University (XJTLU) under the agreement with Soochow University. Animal experiments were performed in accordance with relevant national and provincial guidelines. Randomization was applied for animal use and experimental group setup.

Induction and recording of CSD by electrophysiology in rats and experimental design

Rats were anesthetized with isoflurane in O_2: N_2O (1:2) while breathing spontaneously. The depth of anesthesia was monitored by observing reflexive responses of rats and electroencephalogram (EEG) signals recorded by a digital oscilloscope (DS1000B, RIGOL, Beijing, China) to avoid animal suffering. Two burr holes were drilled on the right skull: a posterior hole (coordinate: 5 mm posterior and 2 mm lateral to bregma) was used for CSD induction and an anterior hole (coordinate: 3 mm anterior and 2 mm lateral to bregma) for implanting a Ag/AgCl electrode (0.1 mm, Applied Neuroscience, London, UK), followed by CSD recording. A grounded reference electrode was placed under the scalp and the extracellular direct current (DC) potential was generated between the reference and recording electrodes for CSD signal. After stabilization for 1-hour post-surgery, CSD was induced by topical application of 2 M KCl for 5 minutes which typically elicits one CSD wave, followed by washing off with artificial cerebrospinal fluid (ACSF, composition in mM: 2.5 NaCl, 250 KCl, 1.18 $MgCl_2$, 1.26 $CaCl_2$; pH 7.35 - 7.45).

The generated EEG and DC signals were first amplified with a AC/DC pre-amplifier (NL834) and then with a AC/DC amplifier (NL106) to gain 5000 × and 250 × amplification respectively. The EEG signal at 1 - 30 Hz and DC signal at 0 - 30 Hz were collected by a filter (NL125). All electrophysiological equipment were purchased from Digitimer (Welwyn Garden City, UK). All signals were digitized and displayed via Labview 11.0 (National Instruments, Austin, TX, USA). As reported previously [20], CSD latency (duration from KCl application to the start of the rising phase of CSD) and

propagation rate were calculated to reflect cortical susceptibility to CSD *in vivo*.

An earlier study reported that inhibition of P2X7 receptor pore complex reduced CSD susceptibility and CSD-induced neuroinflammation in rodents [10]. In this study, we studied whether deactivation of SFKs systematically could similarly reduce cortical susceptibility to CSD and CSD-induced neuroinflammation in rats. Previously, we found that deactivation of SFKs by a SFKs inhibitor PP2 via intracerebroventricular injection reduced cortical susceptibility to CSD in rats [21], suggesting that cortical SFKs plays a crucial role in mediating CSD. However, intracerebroventricular injection is not a clinically applicable route of administration and thus could not provide if SFKs inhibitor is a potential feasible treatment for migraineurs. In order to resolve that issue and show if peripheral injection of modulating SFKs might also have a role in CSD, here we examined if systematic deactivation of SFKs by PP2 affects CSD in rats by investigating the effects of a SFKs inhibitor, PP2 (1407, Tocris, Bristol, UK), or its negative analog, PP3 (2794, Tocris, Bristol, UK) on CSD and CSD-induced IL-1β and TNFα mRNA level in rat cortices ipsilateral to CSD. Each rat was administered with respective drug twice via intraperitoneal injection (*i.p*) for two consecutive days. Surgery was carried Immediately following the 2nd *i.p* injection for a single CSD induction. Rats were divided into four groups: (i) 2% DMSO (vehicle) without 2 M KCl application; (ii) 2% DMSO with KCl application; (iii) 1mg/kg PP2 with KCl application; (iv) 1mg/Kg PP3 with KCl application (n = 7 for each). After CSD recording, rats were sacrificed immediately, and ipsilateral cerebral cortices were collected for subsequent detecting IL-1β and TNFα mRNA level.

Induction and recording of CSD by intrinsic optical imaging in mouse brain slices and experimental design

The complete procedure of this experiment can be referred in our previous publication [20]. Briefly, mouse brain slices at 400 μm of thickness were prepared using a vibratome (7000 smz-2, Campden Instruments, Oxford, UK). Each brain slice was placed in a chamber perfused with Kreb's solution (composition in mM: 126 NaCl, 2.5

KCl, 2.4 $CaCl_2$•$2H_2O$, 1.3 $MgCl_2$•$6H_2O$, 18 $NaHCO_3$; 1.2 NaH_2PO_4, 10 glucose, pH 7.35 – 7.45). CSD was induced on somatosensory cortex by ejection of 260 mM KCl. Intrinsic optical images of the brain slice were continuously recorded for 15 minutes by a monochrome camera (Rolera-XR, ROL-XR-F-M-12, Qimaging, Media Cybernetics, Marlow, UK), which was synchronized with the LED spotlight (SLS-0307-A, Mightex, Pleasanton, CA, USA) via a LED controller (SLC-SA04US, Mightex, Pleasanton, CA, USA). Image Pro Plus software (IPP7.0, Media Cybernetics, Shanghai, China) was used to merge all captured images in which a propagated CSD wave front can be seen. An area of interest (AOI) was selected in the images and a biphasic CSD curve was generated by plotting averaged grey level within the AOI against time. Cortical susceptibility to CSD was represented by CSD latency (the time that takes for a CSD wave propagating to the AOI from the site of KCl ejection) and propagation rate.

Three series of studies were designed using this *in vitro* CSD model.

Series 1: In order to study whether modulation of SFKs activity and P2X7 receptor could similarly regulate cortical susceptibility to CSD, effects of a SFKs inhibitor, saracatinib (S1006, Selleckchem, Houston, USA), that is currently investigated in clinical trials for treating several neurological disorders [22], and a P2X7 receptor antagonist, A740003 (3701, Tocris, Bristol, UK), on CSD latency and propagation rate were examined respectively in C57BL/6J mice brain slices. In this series, three groups were designed as follows: (i) 0.03% DMSO (vehicle) (n = 8); (ii) 0.5 μM saracatinib (n = 8). (iii) 3 μM A740003 (n = 8). It should be noted that two P2X7 receptor antagonists, brilliant blue G, a noncompetitive P2X7 receptor antagonist, and A438079, a competitive antagonist with higher potency and selectivity [23], were previously shown to reduce cortical susceptibility to CSD in rodents [10]. A740003 was applied in this study as it is another potent and highly specific P2X7 receptor competitive antagonist [24] that inhibit both the channel and pore formation. Additionally, this drug is more effective than A438079 in blocking the P2X7 receptor agonist BzATP-induced IL-1β release and pore formation in human cells [24], and in blocking spinal nerve ligation-induced mechanical allodynia [25].

Series 2: Using the mouse brain slice CSD model, we next investigated whether disruption of P2X7 receptor-SFKs interaction could reduce cortical susceptibility to CSD, CSD-induced neuroinflammation and glutamate release. TAT-P2X7 (SLHDSPPTPGQGGGYKKRRQRRR) is a peptide that mimics the Src homology 3 (SH3) domain binding site of the COOH terminus of P2X7 receptor, which disrupts the binding between P2X7 receptor and SFKs [16]. This drug specifically blocks P2X7 receptor pore formation without affecting the cation channel activity [26]. In this series, two groups were designed: (i) 3 μM TAT-P2X7 (n = 8); (ii) 3 μM TAT-P2X7SC (HSPLDSPPQTGGGGYKKRRQRRR), the scrambled control of TAT-P2X7 (n = 8). C57BL/6J mice carry a spontaneous P451L mutation in the SFKs binding site of their P2X7 receptor gene, causing less SFKs binding and impaired pore formation in these mice. Therefore, in this series, Balb/c instead of C57BL/6J mice were used because Balb/c mice carry a fully functional P2X7 receptor without such mutation [27, 28]. Immediately following CSD recording, the brain slices were collected for measuring IL-1β and TNFα mRNA level by qPCR and the media in the chamber during CSD recording were collected for measuring glutamate release using glutamate assay.

Series 3: As P2X7 receptor exhibits functional interaction with NMDA receptor in neurons and a rat epilepsy model [29, 30], while SFKs regulate NMDA receptor activity and function [31], both of which are required for CSD propagation [8, 32, 33], we then explored the involvement of NMDA receptor in SFKs-mediated P2X7 receptor signaling during CSD.

First, we examined if the NMDA receptor agonist, NMDA could reverse the inhibitory effects of TAT-P2X7 on CSD in Balb/c mice brain slices. Two groups were designed: (i) 3 μM TAT-P2X7 (n = 8); (ii) 3 μM TAT-P2X7 + 10 μM NMDA (M3262, Sigma-Aldrich, St. Louis, MO, USA) (n = 8). Immediately following CSD recording, the brain slices were collected for measuring IL-1β mRNA level by qPCR.

Next, we tested whether NMDA receptor-Fyn or -Src interaction mediates cortical susceptibility to CSD in C57BL/6J mice brain slices. Two peptides that specifically block the binding of Fyn or Src from NMDA receptor complex and the Fyn- or Src-

dependent NMDA receptor activity [34, 35] were applied: TAT-Fyn (39-57) (YPSFGVTSIPNYNNFHAAGYGRKKRRQRRR) or TAT-Src(40-49) (KPASADGHRGYGRKKRRQRRR), and their scrambled controls, TAT-Fyn (39-57)SC (PSAYGNPGSAYFNFTNVHIYGRKKRRQRRR) or TAT-Src (40-49)SC (GAAKRPSDGHYGRKKRRQRRR). Of these, TAT-Fyn (39-57) and TAT-Src (40-49) were synthesized peptides that correspond to the amino acids 39-57 and 40-49 of the unique domain of Fyn and Src respectively [34, 35]. Experiments were designed in this part as follows: (i) 1 μM TAT-Fyn (39-57) or 1 μM TAT-Src (40-49) (n = 7 for each); (ii) 1 μM TAT-Fyn (39-57)SC or 1 μM TAT-Src (40-49)SC (n = 7 for each).

Finally, we studied whether P2X7 receptor agonist, BzATP, could reverse the inhibitory effects of TAT-Fyn (39-57) on CSD in C57BL6/J mice brain slices. Two groups were designed: (i) 1 μM TAT-Fyn (39-57) (n = 7); (ii) 1 μM TAT-Fyn (39-57) + 300 μM BzATP (B6396, Sigma-Aldrich, St. Louis, MO, USA) (n = 7).

For the above series of experiments, all drugs were applied on brain slices for 1 hour until the end of CSD recording. All peptides were customized from A^+ peptide (Shanghai, China).

Quantitative polymerase chain reaction (qPCR)

Total RNA of rat cerebral cortices or mouse brain slices were extracted using TRIZOL reagent (T9424, Sigma-Aldrich, St. Louis, MO, USA), followed by reverse transcription to cDNA using GoScript Reverse Transcription System (A5001, Promega, Madison, WI, USA) in Veriti 96-well Thermal Cycler (Applied Biosystems, Waltham, MA, USA). The levels of IL-1β and TNFα mRNA in rat cerebral cortices or mouse brain slices were detected using GoTaq qPCR Master Mix (A6002, Promega, Madison, WI, USA) in QuantStudio 5 Real-Time PCR System (Applied Biosystems, Waltham, MA, USA). Two housekeeping genes, peptidylprolyl isomerase A (PPIA) and β-actin (ACTB), were used for comparative analysis. Primers used to target these genes were as follows: IL-1β forward 5'ACTACAGGCTCCGAGATGAACAAC3', reverse 5'CCCAAGGCCACAGGTATTTT3'; TNFα forward

5’TGCACCACCATCAAGGACTCAAAT3’, reverse 5’ CCCCGGCCTTCCAAATAAATACAT3’; ACTB forward 5’CTGTCCACCTTCCAGCAGAT3’, reverse 5’CGCAGCTCAGTAACAGTCCG3’; PPIA forward 5’TTGCTGCAGACATGGTCAAC3’, reverse 5’TGTCTGCAAACAGCTCGAAG3’. The levels of IL-1β or TNFα mRNA were normalized to the geometric mean of the mRNA levels of the two housekeeping genes.

Glutamate assay

We next examined whether disruption of P2X7 receptor-SFKs interaction reduces CSD-induced glutamate release in mouse brain slices. The level of glutamate released into the media submerging mouse brain slices was measured using a Glutamate Assay Kit (ab83389, Abcam, Cambridge, UK). Briefly, the media and a series of diluted standard solutions were added into a clear assay plate, followed by incubating with glutamate developer and glutamate enzyme mix at 37℃ for 30 minutes. The optical density (OD) at 450 nm was read using a colorimetric microplate reader (BioTek, Winooski, VT, USA). A standard curve correlating the OD value to the concentration of glutamate in the standard solutions was generated to calculate the concentration of glutamate in the media.

Statistical analysis

Data were analyzed using GraphPad Prism 7.0. A normality test was performed for all data by Shapiro-Wilk test. For comparison between two independent groups, if the data fulfilled the normality, they were presented as mean ± standard error of the mean and analyzed by two-tailed unpaired t-test; if not, they were presented as median (interquartile range) and analyzed by two-tailed Mann-Whitney test. Significant differences were indicated by * $p < 0.05$, ** $p < 0.01$, **** $p < 0.0001$

Results

Systematic inhibition of SFKs activity reduced cortical susceptibility to CSD and CSD-associated neuroinflammation in rat ipsilateral cortices

Similar to the reduced cortical susceptibility to CSD under P2X7 receptor inhibition in both rats and mice as reported previously [10], pre-treatment of 1 mg/ml PP2 via intraperitoneal injection significantly prolonged CSD latency to 4.8 ± 0.6 minutes (p = 0.0095) when compared to that at 2.6 ± 0.3 minutes in PP3 group (n = 7 per group) (Fig. 1c d). On contrast , PP2 decreased CSD propagation rate to 1.8 (0.8) mm/minute (p = 0.0169), when compared to that at 3.4 (1.3) mm/minute in PP3 group (n = 7 per group) respectively (Fig. 1c d). Unlike PP2, PP3 did not significantly alter both CSD latency and propagation rate when compared with that in vehicle group.

We next examined if pretreatment of SFKs inhibitor reduces CSD-induced pro-inflammatory cytokines IL-1β and TNFα mRNA level in rat ipsilateral cerebral cortices. CSD markedly increased both IL-1β and TNFα mRNA to 1.9 ± 0.3 (fold change, p = 0.0029) and 3.7 ± 0.6 (p = 0.0042) respectively compared to their levels at 0.5 ± 0 and 1 ± 0.3 in the absence of CSD. Pretreatment of PP2, but not PP3, attenuated both IL-1β and TNFα mRNA induced by CSD to 1.2 ± 0.3 (fold change, p = 0.0232) and 2.2 ± 0.4 (fold change, p = 0.0217). The mRNA fold change of IL-1β and TNFα are 2.8 ± 0.5 and 4.3 ± 0.6 respectively in PP3 group, which did not differ from those in the vehicle group in the presence of CSD (n = 6 per group, Fig. 1e f).

Inhibition of P2X7 receptor and SFKs activity reduced cortical susceptibility to CSD in mouse brain slices

We then investigated the effects of a highly specific P2X7 receptor competitive antagonist [24], A740003 that inhibits both the channel and pore formation, on CSD latency and propagation rate in mouse brain slices. The results showed that perfusion of 3 μM A740003 significantly prolonged CSD latency to 18.4 ± 1.6 seconds and reduced CSD propagation rate to 4.2 ± 0.6 mm/minute when compared to those at 11.31 ± 0.4 seconds (p = 0.0026) and 5.7 ± 0.2 mm/minute (p = 0.0479) respectively in the vehicle group (n = 8 per group, Fig. 2d e). Similar as A740003, albeit to a slightly smaller extent, 0.5 μM saracatinib also prolonged CSD latency to 15.2 ± 0.9 seconds (p = 0.0031) and reduced CSD propagation rate to 4.8 ± 0.1 mm/minute (p = 0.0014)

compared to those of the respective vehicle group (n = 8 per group, Fig. 2d e).

Disrupting P2X7 receptor-SFKs interaction reduced cortical susceptibility to CSD and CSD-associated neuroinflammation in mouse brain slices

We next explored whether disrupting the interaction between P2X7 receptor and SFKs affects CSD in Balb/c mouse brain slices. Perfusion of 3 μM TAT-P2X7, markedly increased CSD latency to 18.2 ± 1.6 seconds (p = 0.0209) and decreased CSD propagation rate to 3.7 ± 0.5 mm/minute (p = 0.0137) in comparison with those at 13.3 ± 0.9 seconds and 5.3 ± 0.3 mm/minute in the scrambled control peptide of TAT-P2X7SC (n = 8 per group, Fig. 3b c).

Consistent to the reduced cortical susceptibility to CSD, 3 μM TAT-P2X7 also attenuated CSD-induced IL-1β mRNA to 0.9 ± 0.1 (fold change, p = 0.0144) compared to that at 1.5 ± 0.2 in 3 μM TAT-P2X7SC group (n = 8 per group, Fig. 3d e). Unlike IL-1β mRNA, CSD-induced TNFα gene expression was not altered by TAT-P2X7 and their mRNA fold change were 1 ± 0.1 and 0.9 ± 0 (p = 0.1612) in the TAT-P2X7 and TAT-P2X7SC groups respectively.

Disrupting P2X7 receptor-SFKs interaction reduced CSD-associated glutamate release in mouse brain slices

We next examined whether disruption of P2X7 receptor-SFKs interaction reduces CSD-induced glutamate release in mouse brain slices. As expected, 3 μM TAT-P2X7 significantly attenuated CSD-induced glutamate release from mouse brain slices to 6.4 ± 1.1 μM (p = 0.0194), which was lower than that at 16.4 ± 3.2 μM in 3 μM TAT-P2X7SC (n = 7 per group, Fig. 4a).

NMDA reversed the reduced cortical susceptibility to CSD but not CSD-associated neuroinflammation by TAT-P2X7 *in mouse brain slices*

We also explored the mechanism of P2X7 receptor/SFKs pathway in mediating CSD. SFKs are known to also interact with NMDA receptors in mediating CSD, we then

examined whether NMDA application could reverse cortical susceptibility to CSD and CSD-induced neuroinflammation by Tat-P2X7 in mouse brain slices. Perfusion of 10 μM NMDA restored the CSD latency prolonged by 3 μM TAT-P2X7 to 13.1 ± 1.1 seconds from 18.2 ± 1.6 seconds (p = 0.0195). Differently, NDMA did not alter the reduced CSD propagation rate by 3 μM TAT-P2X7 (3.7 ± 0.5 mm/minute in TAT-P2X7 group vs. 4.4 ± 0.6 mm/minute in TAT-P2X7 + NMDA group, p = 0.3411, n = 8 per group, Fig. 4c d). Furthermore, NMDA did not affect the reduced IL-1β mRNA fold change by 3 μM TAT-P2X7 (0.9 ± 0.1 in TAT-P2X7 group vs. 1 ± 0.2 in TAT-P2X7 + NMDA group, p = 0.7088, n = 8 per group, Fig. 4e).

Disrupting NMDA receptor -Fyn interaction, but not -Src, reduced cortical susceptibility to CSD in mouse brain slices

We next examined whether disrupting NMDA receptor-Fyn or -Src interaction affects CSD in mouse brain slices. The results showed that 1 μM TAT-Fyn (39-57) significantly prolonged CSD latency to 18.1 ± 1.9 seconds (p = 0.0076) and reduced CSD propagation rate to 3.6 ± 0.3 mm/minute (p < 0.0001) in comparison with that at 10.9 ± 0.7 seconds and 6.7 ± 0.4 mm/minute respectively in its scrambled control TAT-Fyn (39-57)SC group (n = 7 per group, Fig. 5c d). Unlike TAT-Fyn (39-57), 1 μM TAT-Src (40-49), however, did not affect CSD latency and CSD propagation rate, which was 11.5 ± 0.9 seconds (p = 0.1969) and 2.1 (0.9) mm/minute (p = 0.8182) respectively in TAT-Src (40-49) group and 13.6 ± 1.2 seconds and 2.4 (0.6) mm/minute in TAT-Src (40-49)SC group (n = 6 per group).

BzATP reversed the reduced cortical susceptibility to CSD by TAT-Fyn (39-57) in mouse brain slices

We further studied whether activation of P2X7 receptor could restore the reduced cortical susceptibility to CSD by TAT-Fyn (39-57) in mouse brain slices. 300 μM BzATP restored the prolonged CSD latency and the reduced CSD propagation rate by 3 μM TAT-P2X7 from 18 ± 1.9 seconds and 4.1 ± 0.6 mm/minute to 12.5 ± 1.1 seconds (p = 0.0280) and 6.3 ± 0.2 mm/minute (p < 0.0001) respectively in mouse brain slices (n =

7 per group, Fig. 5c d).

Discussion

Here we show for the first time that SFKs activity is required for P2X7 receptor signaling during CSD propagation and CSD-induced neuroinflammation.

Similar as pharmacological inhibition of P2X7 receptor *in vivo* [10], pretreatment of SFKs inhibitor by PP2 via intraperitoneal administration suppresses cortical susceptibility to CSD in rats (Fig. 1c d). This data is in compatible with our previous finding that SFKs regulate cortical susceptibility to CSD in rats via intracerebroventricular administration of the same inhibitor PP2 [21]. Consistent to the *in vivo* data, in mouse brain slices, both inhibition of P2X7 receptor by A740003 and SFKs activity by the clinical relevant SFKs inhibitor saracatinib showed similar reduction in cortical susceptibility to CSD in mouse brain slices (Fig. 2d e). Interestingly, when the interaction between P2X7 receptor and SFKs is disrupted by a peptide TAT-P2X7 that is known to reduce the activated SFKs bound to P2X7 receptor and P2X7 receptor activation-induced SFKs activation [16], the prolonged CSD latency and reduced CSD propagation rate were also observed (Fig. 3b c). Collectively, these findings suggest an interactive relationship between SFKs and P2X7 receptor in mediating cortical susceptibility to CSD.

TAT-P2X7 only inhibits P2X7 receptor activation induced-pore formation but not P2X7 receptor channel activity [26]. The fact that TAT-P2X7 reduces cortical susceptibility to CSD suggests that SFKs participate in P2X7 receptor pore formation to promote CSD propagation. Indeed, inhibition of SFKs activity is previously reported to reduce P2X7 receptor activation-induced cell membrane permeabilization [16]. Consistently to these evidence, selectively targeting P2X7 receptor pore formation by Brilliant blue FCF, but not selective targeting P2X7 receptor channel by calmidazolium, reduced CSD susceptibility [10]. Additionally, C57BL6/J mice with P451L mutation in their P2X7 receptors and impaired pore formation showed lower CSD susceptibility than Balb/c mice [10]. Taken together, our data pinpoint the significant role of SFKs in regulating

P2X7 receptor during CSD propagation.

CSD is known to trigger neuroinflammation and inhibition of P2X7 receptor pore form attenuates CSD-induced neuroinflammation in rodents, including cortical IL-1β, Cox-2, iNOS mRNA level [10]. Similarly, in the present study, pretreatment of SFKs inhibitor also downregulates CSD-induced ipsilateral cortical IL-1β and TNFα mRNA expression in rats (Fig. 1e f). Interestingly, perfusion of TAT-P2X7 reduces CSD-induced IL-1β mRNA expression in mouse brain slices (Fig. 3d e), supporting that disruption of P2X7 receptor and SFKs interaction reduces CSD-induced cortical IL-1β mRNA expression. These data demonstrate that P2X7 receptor/SFKs signaling contributes to CSD-induced neuroinflammation.

The cell-signaling mechanism of P2X7 receptor-SFKs signaling governing CSD-induced IL-1β gene expression is not well known. Interestingly, a recent finding shows that NF-kappaB-p65 co-express with P2X7 receptor in mice cortical and subcortical structures. In this study, the authors report that CSD induces NF-kappaB-p65 nuclear translocation, which can be reversed by P2X7 receptor antagonist [36]. Consistently, Fyn kinase activity also enhances NF-kappaB-p65 nuclear translocation, which correlates with IL-1β gene expression in a Parkinson' disease model [37]. In the present study, SFKs, in particular Fyn kinase, transmits signaling of P2X7 receptors in CSD and CSD-induced IL-1β gene expression. As such, it is likely that the mechanism of P2X7 receptor-SFKs signaling governing CSD-induced IL-1β gene expression may involve NF-kappaB-p65 nuclear translocation, however, this possibility requires future investigation. It is noted that, unlike the inhibition of SFKs alone in rats (Fig. 1e f), TAT-P2X7 does not alter CSD-induced TNFα mRNA expression in mouse brain slices (Fig. 3d e). It is possible that partial SFKs are still active to promote TNFα mRNA expression via alternative pathways independent of P2X7 receptors.

Albeit the mechanism underlying how SFKs mediate P2X7 receptor signaling during CSD is not fully known, the present study shows involvement of glutamatergic pathway. P2X7 receptor is known to regulate glutamate release from astrocytes and central

brain regions, facilitating glia-neuron communication and the development of neuropathic pain [38, 39]. Here, we show that disruption of P2X7 receptor-SFKs interaction by TAT-P2X7 reduces CSD-induced glutamate release (Fig. 4a). Reciprocally, the TAT-P2X7-reduced cortical susceptibility to CSD can be restored by NMDA (Fig. 4c d). This is consistent with previous findings that both P2X7 receptor and SFKs have functional interaction with NMDA receptor respectively in different models of neurological diseases [29, 30]; Notably, functional interaction between NR2A-containing NMDA receptor and SFKs mediates CSD as evidenced by that the SFK activator, pYEEI restored the inhibitory effect of NR2A-containining NMDA receptor antagonist on CSD in mouse brain slices [21]. These data suggest that P2X7 receptor/SFKs signaling-mediated CSD is likely to be dependent on NMDA receptor activity. Unexpectedly, NMDA does not affect the TAT-P2X7-reduced IL-1β mRNA expression (Fig. 4e), indicating that NMDA receptor may not be involved downstream of P2X7 receptor/SFK signaling in the CSD-induced neuroinflammation. It is noted that disrupting the interaction between NMDA receptor and Fyn, a subtype of SFKs, using a dual P2X7-NMDA receptor antagonist that is developed for treatment of Alzheimer's Disease in order to target both NMDA receptor-mediated neurodegeneration and P2X7 receptor-mediated neuroinflammation [40], reduces cortical susceptibility to CSD (Fig. 5c d). This data implies that Fyn-dependent NMDA receptor activity is required for mediating CSD susceptibility. Unlike disrupting NMDA receptor-Fyn interaction, disrupting the NMDA receptor-Src interaction does not affect CSD (Fig. 5c d). As TAT-Fyn (39-57) and TAT-Src (40-49) specifically block the binding of Fyn or Src from NMDA receptor complex and the Fyn- or Src-dependent NMDA receptor activity [34, 35], these data support that Fyn, but not Src, is required for NMDA receptor-mediated CSD propagation.

In order to confirm the involvement of P2X7 receptor in this process, we further show that activation of P2X7 receptor restores TAT-Fyn (39-57)-reduced cortical susceptibility to CSD (Fig. 5c d). These findings, together with ours, suggest that SFKs-transmitted P2X7 receptor signaling mediates CSD susceptibility via glutamatergic

pathway. Taken together and given that NMDA receptor facilitates CSD initiation and propagation [1, 32], we propose that P2X7 receptor/SFKs signaling promotes cortical susceptibility to CSD and CSD-induced glutamate release, which subsequently may sustain NMDA receptor activity and create a positive feedback loop contributing to CSD-associated migraine pathogenesis.

The mechanism underlying SFKs-mediated P2X7 receptor signaling during CSD is also likely involving Panx1. Our previous study demonstrates that CSD promotes Panx1 and SFKs coupling in cerebral cortices and the interaction between Panx1 and SFKs regulates CSD susceptibility [20]. Similar to P2X7 receptor, SFKs activity also regulate Panx1 activation and channel opening induced by CSD [20]. SFKs are possibly the intermediate protein linking P2X7 receptor and Panx1 to form a functional pore but whether the three proteins form a complex requires further study. Additionally, SFKs often phosphorylate their interacting proteins to regulate their functions and activities. A more recent study identified tyrosine 382-384 within the second transmembrane domain and the intracellular C-terminus of P2X7 receptor as potential tyrosine phosphorylation sites [17]. Whether SFKs can phosphorylate these sites of P2X7 receptor to regulate P2X7 receptor function and signaling awaits to be studied.

Conclusion

In conclusion, our data show that SFKs activity mediates P2X7 receptor during CSD propagation and CSD-induced neuroinflammation. We propose a novel SFKs-transmitted P2X7 signaling that facilitates CSD propagation via glutamatergic pathway (Fig. 6). Our findings provide evidence for potential clinical application of drugs targeting P2X7 receptor/SFKs signaling molecules in migraine prophylaxis and therapy.

DECLARATIONS

Ethics approval and consent to participate:

The study received ethical approval from the Ethic Review Panel of Soochow University and performed in accordance with the relevant national and provincial guidelines. Written informed consent: Not applicable.

Consent for publication:

Not applicable.

Availability of data and materials：

Data reported in this manuscript are available within the article. Raw data materials are available with the Corresponding author, which can be readily accessed by the Journal upon request.

Competing interests:

The authors declare that they have no competing interests.

Funding:

This paper was supported by Key Program Special Fund in XJTLU (KSF-E-08).

Authors' contributions:

L.N and D.M designed, performed experiments, analyzed data and drafted manuscript; J.P Quinn co-supervised L.N and D.M. M.W sponsored, supervised L.N, and D.M designed research and edited the manuscript.

Acknowledgements:

The authors thank all members in the lab at XJTLU for interesting discussions

ARTICLE HIGHLIGHTS

- SFKs activity-mediated P2X7 receptor pore formation facilitates CSD propagation involving glutamatergic pathway and CSD-induced neuroinflammation.

- P2X7 receptor and SFKs can be used as targets in migraine prophylaxis and therapy.

Abbreviations

CSD=cortical spreading depression; **SFKs**=Src family kinases; **NMDA**=N-methyl-D-aspartate (NMDA); **CGRP=**calcitonin gene-related peptide; **PACAP=**pituitary adenylate-cyclase-activating polypeptide; **Panx1=**pannexin 1; **NTG=**nitroglycerin; **TNC=**trigeminal nucleus caudalis; **DC=**direct current; **EEG**=electroencephalogram

References

1. Costa C, Tozzi A, Rainero I, Cupini LM, Calabresi P, Ayata C, et al. (2013) Cortical spreading depression as a target for anti-migraine agents. J Headache Pain 14(1):62.
2. Schock SC, Munyao N, Yakubchyk Y, Sabourin LA, Hakim AM, Ventureyra EC, et al. (2007) Cortical spreading depression releases ATP into the extracellular space and purinergic receptor activation contributes to the induction of ischemic tolerance. Brain Res 1168129-38.
3. Waschek JA, Baca SM and Akerman S (2018) PACAP and migraine headache: immunomodulation of neural circuits in autonomic ganglia and brain parenchyma. J Headache Pain 19(1):23.
4. Karatas H, Erdener SE, Gursoy-Ozdemir Y, Lule S, Eren-Koçak E, Sen ZD, et al. (2013) Spreading depression triggers headache by activating neuronal Panx1 channels. Science 339(6123):1092-5.
5. Lauritzen M, Dreier JP, Fabricius M, Hartings JA, Graf R and Strong AJ (2011) Clinical relevance of cortical spreading depression in neurological disorders: migraine, malignant stroke, subarachnoid and intracranial hemorrhage, and traumatic brain injury. J Cereb Blood Flow Metab 31(1):17-35.
6. Noseda R and Burstein R (2013) Migraine pathophysiology: anatomy of the trigeminovascular pathway and associated neurological symptoms, CSD, sensitization and modulation of pain. Pain 154 Suppl 1.
7. Tang C, Unekawa M, Kitagawa S, Takizawa T, Kayama Y, Nakahara J, et al. (2020) Cortical spreading depolarisation-induced facial hyperalgesia, photophobia and hypomotility are ameliorated by sumatriptan and olcegepant. Sci Rep 10(1):11408.
8. Marrannes R, Willems R, De Prins E and Wauquier A (1988) Evidence for a role of the N-methyl-D-aspartate (NMDA) receptor in cortical spreading depression in the rat. Brain Res 457(2):226-40.
9. Holland PR, Akerman S and Goadsby PJ (2010) Cortical spreading depression-associated cerebral blood flow changes induced by mechanical stimulation are modulated by AMPA and GABA receptors. Cephalalgia 30(5):519-27.
10. Chen SP, Qin T, Seidel JL, Zheng Y, Eikermann M, Ferrari MD, et al. (2017) Inhibition

of the P2X7-PANX1 complex suppresses spreading depolarization and neuroinflammation. Brain 140(6):1643-1656.

11. Jiang L, Wang Y, Xu Y, Ma D and Wang M (2018) The Transient Receptor Potential Ankyrin Type 1 Plays a Critical Role in Cortical Spreading Depression. Neuroscience 38223-34.
12. Mishra A, Behura A, Kumar A, Naik L, Swain A, Das M, et al. (2021) P2X7 receptor in multifaceted cellular signalling and its relevance as a potential therapeutic target in different diseases. Eur J Pharmacol 906174235.
13. Locovei S, Scemes E, Qiu F, Spray DC and Dahl G (2007) Pannexin1 is part of the pore forming unit of the P2X(7) receptor death complex. FEBS Lett 581(3):483-8.
14. Gölöncsér F and Sperlágh B (2014) Effect of genetic deletion and pharmacological antagonism of P2X7 receptors in a mouse animal model of migraine. J Headache Pain 15(1):24.
15. Jiang L, Zhang Y, Jing F, Long T, Qin G, Zhang D, et al. (2021) P2X7R-mediated autophagic impairment contributes to central sensitization in a chronic migraine model with recurrent nitroglycerin stimulation in mice. J Neuroinflammation 18(1):5.
16. Iglesias R, Locovei S, Roque A, Alberto AP, Dahl G, Spray DC, et al. (2008) P2X7 receptor-Pannexin1 complex: pharmacology and signaling. Am J Physiol Cell Physiol 295(3):C752-60.
17. Leduc-Pessah H, Weilinger NL, Fan CY, Burma NE, Thompson RJ and Trang T (2017) Site-Specific Regulation of P2X7 Receptor Function in Microglia Gates Morphine Analgesic Tolerance. J Neurosci 37(42):10154-10172.
18. Bianco F, Perrotta C, Novellino L, Francolini M, Riganti L, Menna E, et al. (2009) Acid sphingomyelinase activity triggers microparticle release from glial cells. Embo j 28(8):1043-54.
19. Martel-Gallegos G, Casas-Pruneda G, Ortega-Ortega F, Sánchez-Armass S, Olivares-Reyes JA, Diebold B, et al. (2013) Oxidative stress induced by P2X7 receptor stimulation in murine macrophages is mediated by c-Src/Pyk2 and ERK1/2. Biochim Biophys Acta 1830(10):4650-9.
20. Bu F, Nie L, Quinn JP and Wang M (2020) Sarcoma Family Kinase-Dependent Pannexin-1 Activation after Cortical Spreading Depression is Mediated by NR2A-Containing Receptors. Int J Mol Sci 21(4):1296.
21. Bu F, Wang Y, Jiang L, Ma D, Quinn JP and Wang M (2018) Sarcoma family kinase activity is required for cortical spreading depression. Cephalalgia 38(11):1748-1758.
22. Nie L, Ye WR, Chen S, Chirchiglia D and Wang M (2021) Src Family Kinases in the Central Nervous System: Their Emerging Role in Pathophysiology of Migraine and Neuropathic Pain. Curr Neuropharmacol 19(5):665-678.
23. Donnelly-Roberts DL and Jarvis MF (2007) Discovery of P2X7 receptor-selective antagonists offers new insights into P2X7 receptor function and indicates a role in chronic pain states. Br J Pharmacol 151(5):571-9.
24. Honore P, Donnelly-Roberts D, Namovic MT, Hsieh G, Zhu CZ, Mikusa JP, et al. (2006) A-740003 [N-(1-{[(cyanoimino)(5-quinolinylamino) methyl]amino}-2,2-dimethylpropyl)-2-(3,4-dimethoxyphenyl)acetamide], a novel and selective P2X7 receptor antagonist, dose-dependently reduces neuropathic pain in the rat. J Pharmacol Exp Ther

319(3):1376-85.
25. Honore P, Wade CL, Zhong C, Harris RR, Wu C, Ghayur T, et al. (2006) Interleukin-1alphabeta gene-deficient mice show reduced nociceptive sensitivity in models of inflammatory and neuropathic pain but not post-operative pain. Behav Brain Res 167(2):355-64.
26. Sorge RE, Trang T, Dorfman R, Smith SB, Beggs S, Ritchie J, et al. (2012) Genetically determined P2X7 receptor pore formation regulates variability in chronic pain sensitivity. Nat Med 18(4):595-9.
27. Adriouch S, Dox C, Welge V, Seman M, Koch-Nolte F and Haag F (2002) Cutting edge: a natural P451L mutation in the cytoplasmic domain impairs the function of the mouse P2X7 receptor. J Immunol 169(8):4108-12.
28. Le Stunff H, Auger R, Kanellopoulos J and Raymond MN (2004) The Pro-451 to Leu polymorphism within the C-terminal tail of P2X7 receptor impairs cell death but not phospholipase D activation in murine thymocytes. J Biol Chem 279(17):16918-26.
29. Laties CHMMZXZWLDRAM (2006) Neuronal Death Evoked by the P2X7 Receptor Mediated by the NMDA Receptor. Investig Ophthalmol Vis Sci 47(13):2589.
30. Doğan E, Aygün H, Arslan G, Rzayev E, Avcı B, Ayyıldız M, et al. (2020) The Role of NMDA Receptors in the Effect of Purinergic P2X7 Receptor on Spontaneous Seizure Activity in WAG/Rij Rats With Genetic Absence Epilepsy. Front Neurosci 14414.
31. Salter MW and Kalia LV (2004) Src kinases: a hub for NMDA receptor regulation. Nat Rev Neurosci 5(4):317-28.
32. Bu F, Du R, Li Y, Quinn JP and Wang M (2016) NR2A contributes to genesis and propagation of cortical spreading depression in rats. Sci Rep 623576.
33. Peeters M, Gunthorpe MJ, Strijbos PJ, Goldsmith P, Upton N and James MF (2007) Effects of pan- and subtype-selective N-methyl-D-aspartate receptor antagonists on cortical spreading depression in the rat: therapeutic potential for migraine. J Pharmacol Exp Ther 321(2):564-72.
34. Yang K, Trepanier C, Sidhu B, Xie YF, Li H, Lei G, et al. (2012) Metaplasticity gated through differential regulation of GluN2A versus GluN2B receptors by Src family kinases. Embo J 31(4):805-16.
35. Liu XJ, Gingrich JR, Vargas-Caballero M, Dong YN, Sengar A, Beggs S, et al. (2008) Treatment of inflammatory and neuropathic pain by uncoupling Src from the NMDA receptor complex. Nat Med 14(12):1325-32.
36. Uzay B, Donmez-Demir B, Yilmaz-Ozcan S, Eren-Kocak E, Yemisci M, Dalkara T, et al. (2021) The Effects of P2X7 Antagonism on Neuroinflammation Following Optogenetically-Triggered Cortical Spreading Depression. J Headache Pain 22(103):14 (AL037).
37. Panicker N, Sarkar S, Harischandra DS, Neal M, Kam TI, Jin H, et al. (2019) Fyn kinase regulates misfolded α-synuclein uptake and NLRP3 inflammasome activation in microglia. J Exp Med 216(6):1411-1430.
38. Duan S, Anderson CM, Keung EC, Chen Y, Chen Y and Swanson RA (2003) P2X7 receptor-mediated release of excitatory amino acids from astrocytes. J Neurosci 23(4):1320-8.
39. Andó RD and Sperlágh B (2013) The role of glutamate release mediated by

extrasynaptic P2X7 receptors in animal models of neuropathic pain. Brain Res Bull 9380-5.

40. Karoutzou O, Kwak SH, Lee SD, Martínez-Falguera D, Sureda FX, Vázquez S, et al. (2018) Towards a Novel Class of Multitarget-Directed Ligands: Dual P2X7-NMDA Receptor Antagonists. Molecules 23(1).

Figure 1. Systematic deactivation of SFKs reduced cortical susceptibility to CSD and CSD-associated neuroinflammation in rat ipsilateral cortices. **a** Schematic presentation of cranial preparation and *in vivo* experimental protocol. **b** Representative traces of CSD affected by 1mg/kg PP2 and PP3. **c d** Effects of vehicle, 1mg/ml PP2 and PP3 on CSD latency and propagation rate. **e f** Effects of vehicle, 1mg/ml PP2 and PP3 on CSD-induced IL-1β and TNFα mRNA fold change in rat ipsilateral cerebral cortices. Two-tailed unpaired t-test was used for comparison in CSD latency between PP2 and PP3 group, in IL-1β and TNFα mRNA fold change between vehicle without CSD and vehicle with CSD group, PP2 and PP3 groups with CSD. Two-tailed Mann-Whitney test was used for comparison in CSD propagation rate between PP2 and PP3 group.

Figure 2. Both deactivation of P2X7 receptor and SFKs reduced cortical susceptibility to CSD in mouse brain slices. **a** The captured images of a mouse brain slice before and after CSD induction by 260 mM KCl in cerebral cortex. The arrow indicated the direction of CSD propagation. An AOI was selected and kept the same for data analysis. **b** The biphasic CSD curve generated from the images recorded for 15 minutes by plotting averaged grey level within the AOI against time. CSD latency (sec) is the time interval between KCl application and CSD elicitation at the AOI. CSD propagation rate (mm/min) is the velocity by which CSD propagates along cerebral cortex. **c** Representative traces of the 1st peak of CSD affected by vehicle (Veh), 3 μM A740003 and 0.5 μM saracatinib. Only the trace recorded during the first 100 seconds was displayed here in order to clearly show the starting points of KCl application and CSD elicitation. **d e** Effects of vehicle, 3 μM A740003 and 0.5 μM saracatinib on CSD latency and propagation rate. Abbreviations: vehicle (Veh); saracatinib (SRCT); seconds (sec); mm/minute (mm/min). Two-tailed unpaired t-test was used for comparison between vehicle and A740003 group, vehicle and saracatinib group.

Figure 3. Disrupting P2X7 receptor-SFKs interaction reduced cortical susceptibility to CSD and CSD-associated neuroinflammation in mouse brain slices. **a** Representative traces of 1st peak of CSD affected by 3 μM TAT-P2X7 and TAT-P2X7SC. Only the trace recorded during the first 100 seconds was displayed here in order to clearly show CSD latency in respective group. **b c** Effects of 3 μM TAT-P2X7 and TAT-P2X7SC on CSD latency and propagation rate. **d e** Effects of 3 μM TAT-P2X7 and TAT-P2X7SC on CSD-induced IL-1β and TNFα mRNA fold change in mouse brain slices. Two-tailed unpaired t-test was used for comparison between TAT-P2X7 and TAT-P2X7SC group.

Figure 4. Activation of NMDA receptor restored the disrupted P2X7 receptor-SFKs interaction-reduced cortical susceptibility to CSD but not CSD-associated neuroinflammation in mouse brain slices. **a** Effects of 3 μM TAT-P2X7 and TAT-P2X7SC on CSD-induced glutamate release in mouse brain slices. **b** Representative traces of 1st peak of CSD affected by 3 μM TAT-P2X7 and 3 μM TAT-P2X7 + 10 μM NMDA. **c d** Effects of 3 μM TAT-P2X7 and 3 μM TAT-P2X7 + 10 μM NMDA on CSD latency and propagation rate. **e** Effect of 3 μM TAT-P2X7 + 10 μM NMDA on CSD-induced IL-1β mRNA fold change in mouse brain slices. Two-tailed unpaired t-test was used for comparison between TAT-P2X7 and TAT-P2X7 + NMDA group.

Figure 5. Disrupting NMDA receptor-Fyn but not -Src interaction reduced cortical susceptibility to CSD in mouse brain slices. **a b** Representative traces of 1st peak of CSD affected by 1 μM TAT-Fyn (39-57), 1 μM TAT-Fyn (39-57)SC, 1 μM TAT-Fyn (39-57) + 300 μM BzATP, 1 μM TAT-Src (40-49) and 1 μM TAT-Src (40-49)SC. **c d** Effects of 1 μM TAT-Fyn (39-57), 1 μM TAT-Fyn (39-57)SC, 1 μM TAT-Fyn (39-57) + 300 μM BzATP, 1 μM TAT-Src (40-49) and 1 μM TAT-Src (40-49)SC on CSD latency and propagation rate. Two-tailed unpaired t-test was used for comparison in CSD latency between TAT-Fyn (39-57) and TAT-Fyn (39-57)SC group, TAT-Fyn (39-57) and TAT-Fyn (39-57) + BzATP group, TAT-Src (40-49) and TAT-Src (40-49)SC group, in CSD propagation rate between TAT-Fyn (39-57) and TAT-Fyn (39-57)SC group, TAT-Fyn

(39-57) and TAT-Fyn (39-57) + BzATP group. Two-tailed Mann-Whitney test was used for comparison in CSD propagation rate between TAT-Src (40-49) and TAT-Src (40-49)SC group.

Figure 6. Schematic representation of the role that P2X7 receptor/SFKs signaling may exert in CSD-associated migraine pathophysiology. P2X7 receptor/SFKs signaling is activated during CSD to facilitate neuroinflammation, NMDA receptor activation and glutamate release, among which, glutamate may in return reinforce the activation of NMDA receptor (dotted line with arrow) and facilitate cortical susceptibility, forming a positive loop.

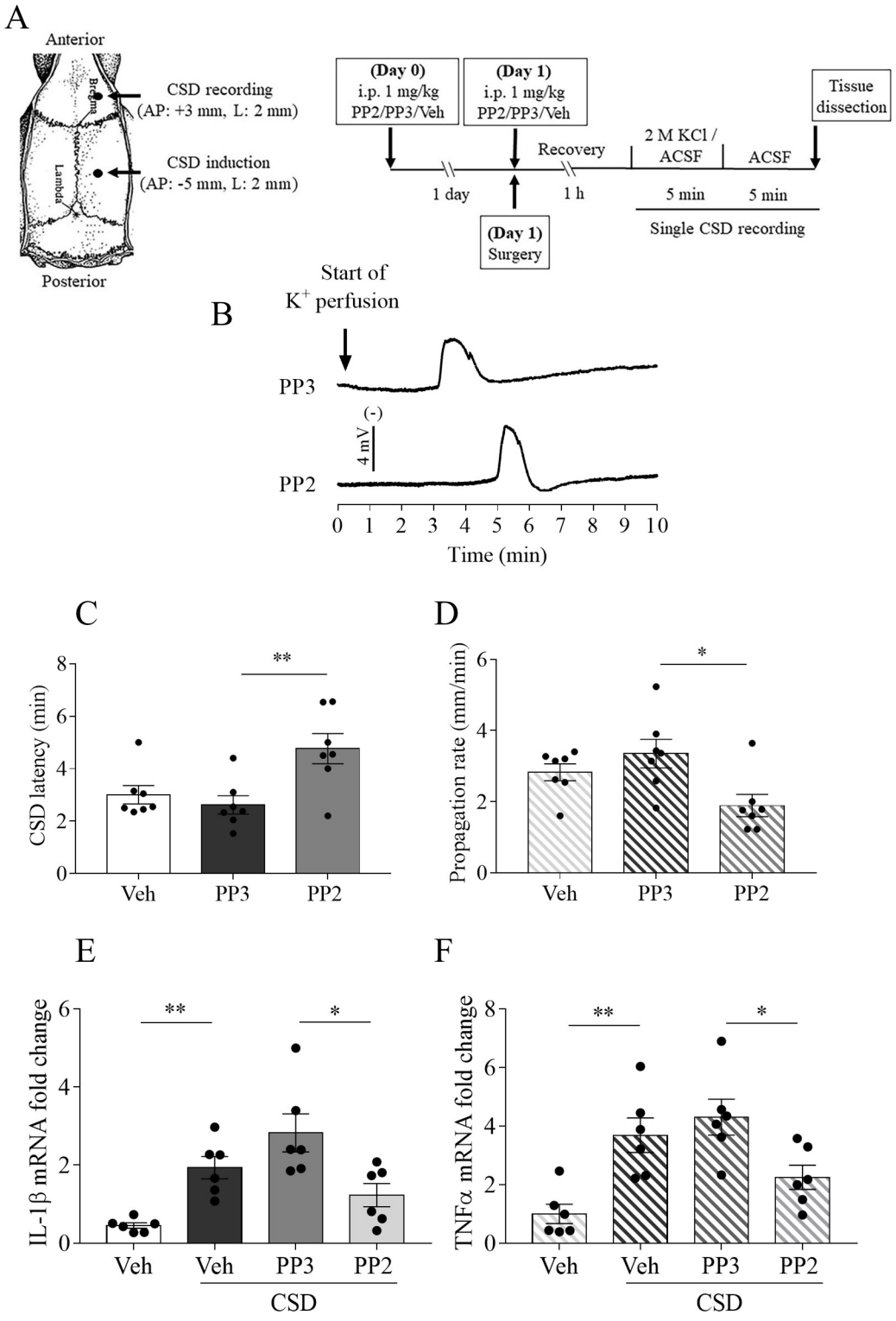
A
Anterior
Posterior
Bregma
Lambda
CSD recording
(AP: +3 mm, L: 2 mm)
CSD induction
(AP: -5 mm, L: 2 mm)
(Day 0)
i.p. 1 mg/kg
PP2/PP3/Veh
(Day 1)
i.p. 1 mg/kg
PP2/PP3/Veh
Tissue
dissection
Recovery
2 M KCl /
ACSF
ACSF
1 day
1 h
5 min
5 min
(Day 1)
Surgery
Single CSD recording
B
Start of
K+ perfusion
PP3
PP2
(-)
4 mV
0 1 2 3 4 5 6 7 8 9 10
Time (min)
C
CSD latency (min)
**
Veh
PP3
PP2
D
Propagation rate (mm/min)
*
Veh
PP3
PP2
E
IL-1β mRNA fold change
**
*
Veh
Veh
PP3
PP2
CSD
F
TNFα mRNA fold change
**
*
Veh
Veh
PP3
PP2
CSD

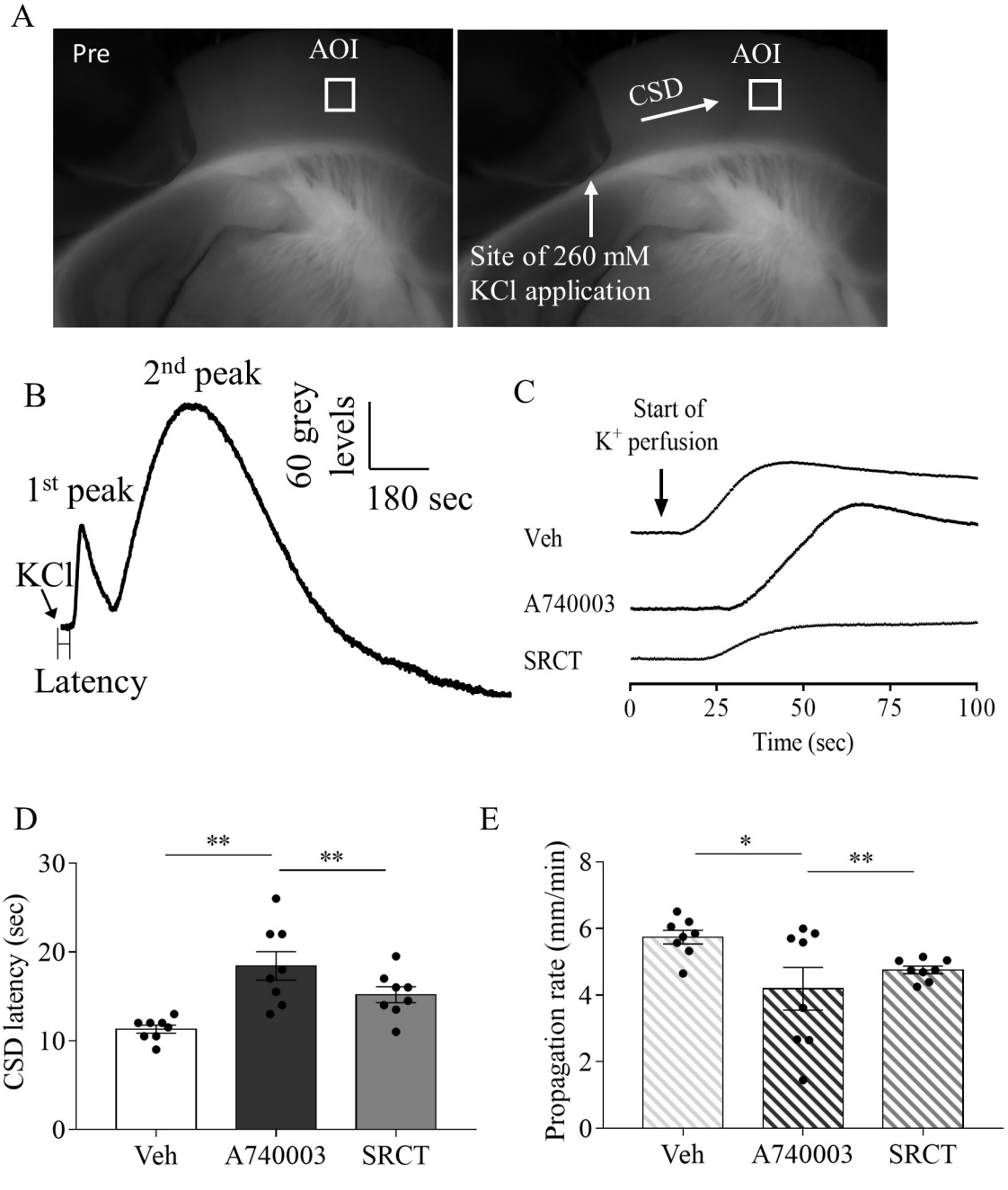
A
Pre
AOI
AOI
CSD
Site of 260 mM
KCl application
B
2nd peak
1st peak
60 grey
levels
180 sec
KCl
Latency
C
Start of
K+ perfusion
Veh
A740003
SRCT
0
25
50
75
100
Time (sec)
D
CSD latency (sec)
30
20
10
0
**
**
Veh
A740003
SRCT
E
Propagation rate (mm/min)
8
6
4
2
0
*
**
Veh
A740003
SRCT

Fig.3

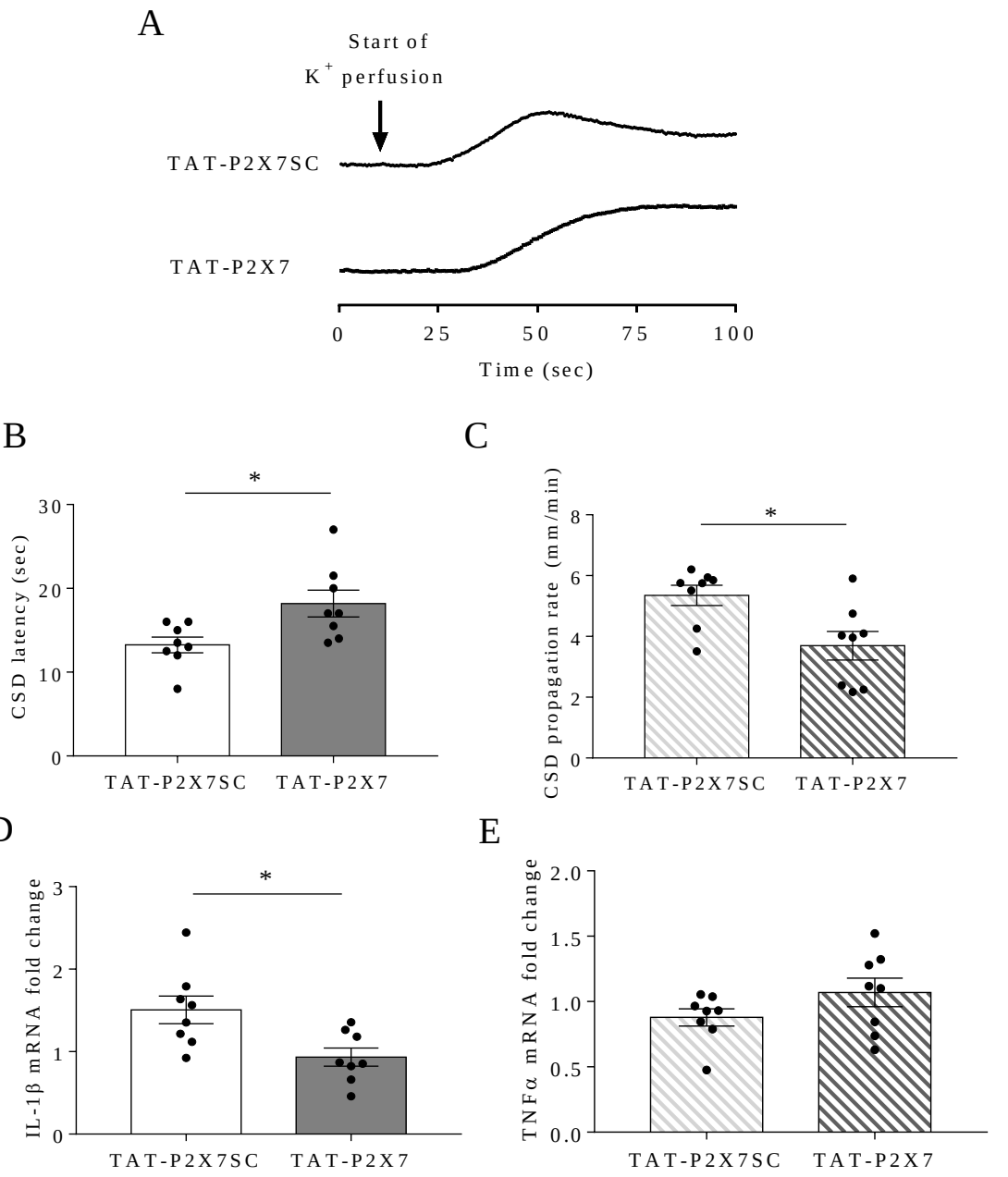
A
Start of
K+ perfusion
TAT-P2X7SC
TAT-P2X7
0
25
50
75
100
Time (sec)
B
CSD latency (sec)
30
20
10
0
*
TAT-P2X7SC
TAT-P2X7
C
CSD propagation rate (mm/min)
8
6
4
2
0
*
TAT-P2X7SC
TAT-P2X7
D
IL-1β mRNA fold change
3
2
1
0
*
TAT-P2X7SC
TAT-P2X7
E
TNFα mRNA fold change
2.0
1.5
1.0
0.5
0.0
TAT-P2X7SC
TAT-P2X7

Fig. 4

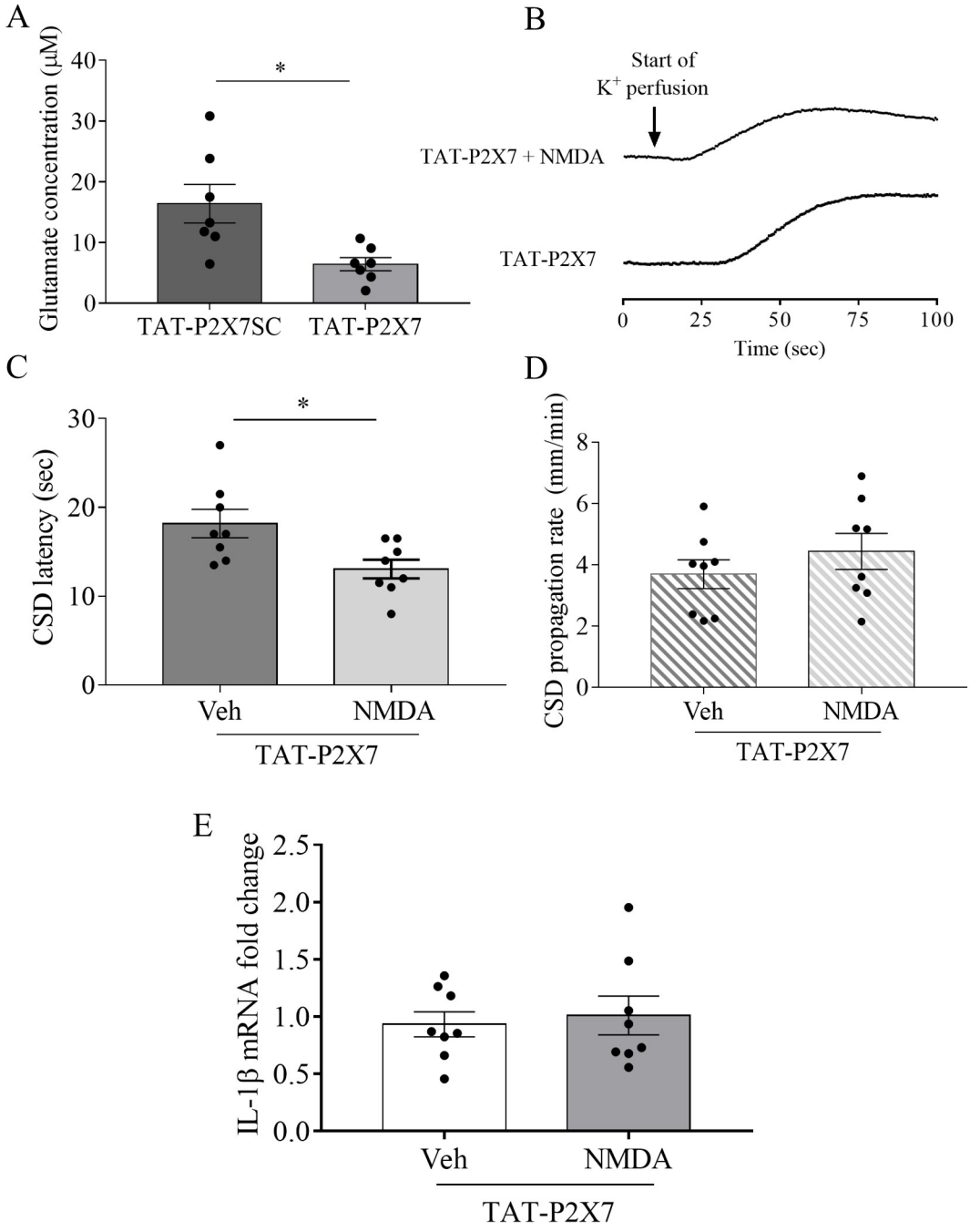
A
Glutamate concentration (μM)
40
30
20
10
0
*
TAT-P2X7SC
TAT-P2X7
B
Start of
K+ perfusion
TAT-P2X7 + NMDA
TAT-P2X7
0
25
50
75
100
Time (sec)
C
CSD latency (sec)
30
20
10
0
*
Veh
NMDA
TAT-P2X7
D
CSD propagation rate (mm/min)
8
6
4
2
0
Veh
NMDA
TAT-P2X7
E
IL-1β mRNA fold change
2.5
2.0
1.5
1.0
0.5
0.0
Veh
NMDA
TAT-P2X7

Fig.5

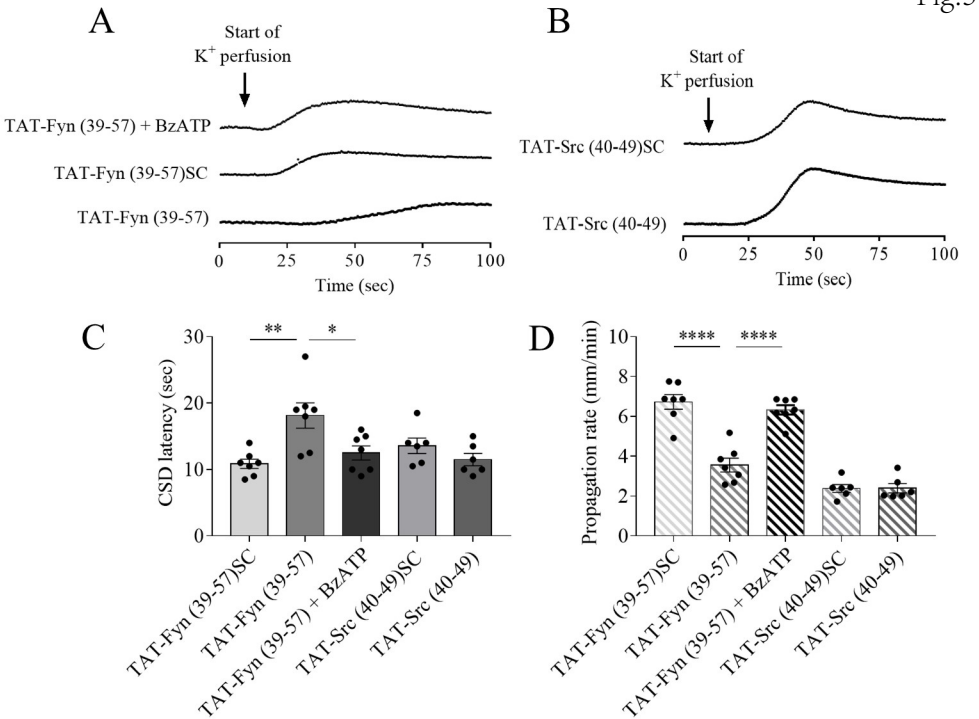
A
Start of
K+ perfusion
TAT-Fyn (39-57) + BzATP
TAT-Fyn (39-57)SC
TAT-Fyn (39-57)
0
25
50
75
100
Time (sec)
B
Start of
K+ perfusion
TAT-Src (40-49)SC
TAT-Src (40-49)
0
25
50
75
100
Time (sec)
C
CSD latency (sec)
30
20
10
0
**
*
TAT-Fyn (39-57)SC
TAT-Fyn (39-57)
TAT-Fyn (39-57) + BzATP
TAT-Src (40-49)SC
TAT-Src (40-49)
D
Propagation rate (mm/min)
10
8
6
4
2
0
****
****
TAT-Fyn (39-57)SC
TAT-Fyn (39-57)
TAT-Fyn (39-57) + BzATP
TAT-Src (40-49)SC
TAT-Src (40-49)

Fig.6

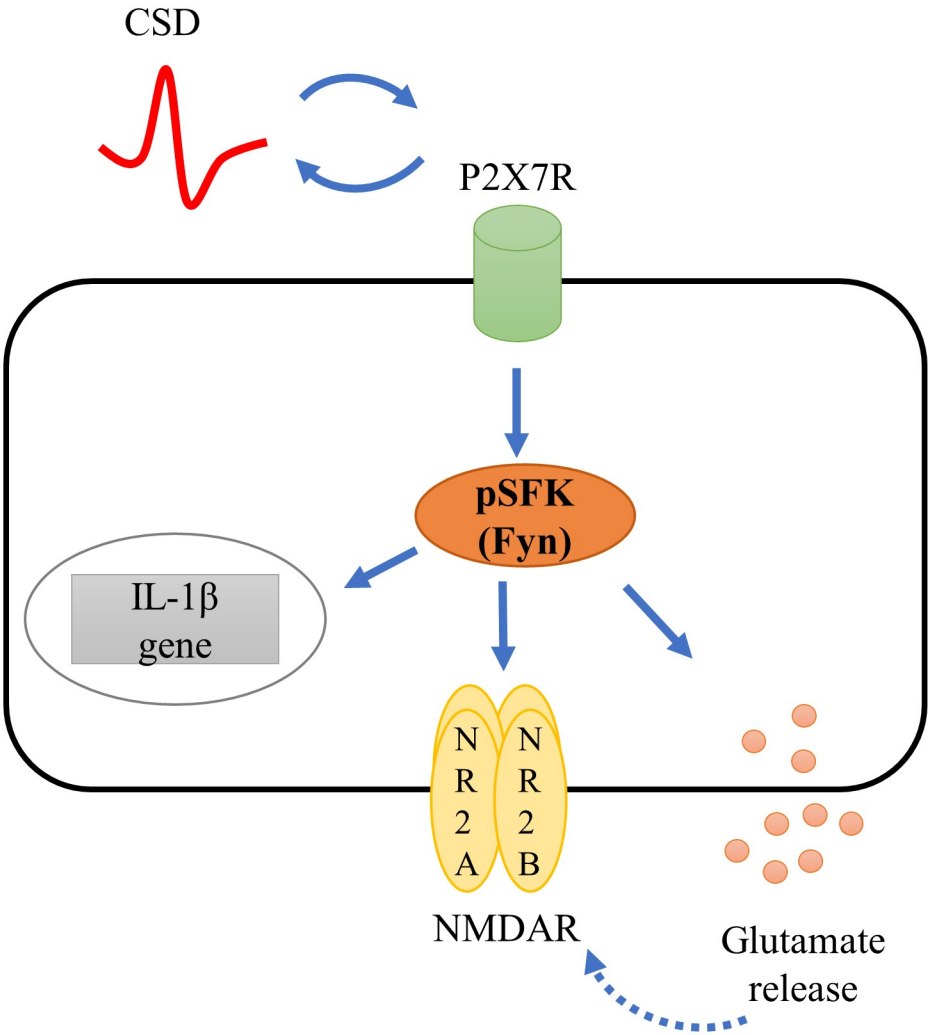
CSD
P2X7R
pSFK
(Fyn)
IL-1β
gene
N
R
2
A
N
R
2
B
NMDAR
Glutamate
release